PHILOSOPHICAL TRANSACTIONS OF THE ROYAL SOCIETY A MATHEMATICAL, PHYSICAL & ENGINEERING SCIENCES

Theoretical Aspects of Electron Energy Loss Spectroscopy

D. L. Mills and S. Y. Tong

Phil. Trans. R. Soc. Lond. A 1986 **318**, 179-198
doi: 10.1098/rsta.1986.0070

Phil. Trans. R. Soc. Lond. A **318**, 179–198 (1986) [179]
Printed in Great Britain

Theoretical aspects of electron energy loss spectroscopy

By D. L. Mills[1] and S. Y. Tong[2]

[1] *Department of Physics, University of California, Irvine, California* 92715, *U.S.A.*
[2] *Department of Physics, University of Wisconsin–Milwaukee, Milwaukee, Wisconsin* 54301, *U.S.A.*

The technique of electron energy loss spectroscopy has provided us with a large body of data on the vibrational normal modes of atoms and molecules adsorbed on crystal surfaces, and of atoms within the outermost surface layers of crystals. In this paper, we review the theoretical description of the inelastic scattering events studied by the method, with emphasis on a series of recent calculations directed at a quantitative description of scattering events in which the electron emerges far from the specular direction or that of a Bragg beam, as a consequence of exciting a vibrational mode of short wavelength.

1. General introduction

In both molecular and solid state physics, knowledge of vibrational spectra is of crucial importance. The array of frequencies tells us about both the nature of the chemical bonds present and places constraints on the structural arrangement of the basic entities, and selection rules associated with the various spectroscopies aid in the identification of the normal modes studied and lead to powerful limitations on the geometry of the system under study.

Generally, infrared and Raman spectroscopy, with their complementary selection rules, suffice for the study of molecular vibrations. The vibrational spectra of crystals are far more complex than those of simple molecules (Born & Huang 1954). The normal modes are wave-like excitations characterized by a wavevector $\boldsymbol{Q}$, confined to a certain geometrical construction called the first Brillouin zone. The first Brillouin zone lies within a polyhedron, whose shape is dictated by the fundamental lattice (the Bravais lattice) upon which the quasimolecular units from which the crystal is built are arranged. If there are z atoms in each structural unit cell of the crystal, then for each value of the wavevector $\boldsymbol{Q}$, there are $3z$ normal modes with frequency $\omega_j(\boldsymbol{Q})$, where the label j ranges from 1 to $3z$.

An ideal spectroscopy of the solid state is one that measures the frequencies of the normal modes throughout the Brillouin zone. Since the wavevector $\boldsymbol{Q}$ is always conserved in an absorption or scattering event, this cannot be done with a spectroscopy that employs infrared or optical-frequency radiation. The magnitude of the wavevector of such a photon is at most 10^5 cm^{-1}, while the Brillouin zone extends out to values typically π/a_0, where a_0 is the lattice constant. Thus, we need a probe that can examine modes with wavevectors as large as 10^8 cm^{-1}; the optical spectroscopies can probe only the region very near the centre of the first Brillouin zone.

Thermal neutrons have wavevectors the order of 10^8 cm^{-1}, and the use of monoenergetic, highly collimated beams of thermal neutrons provided the first detailed data on the phonon dispersion curves of solids. The technique has been used to study the vibrational normal modes of a wide variety of crystals for many years now; other elementary excitations (spin waves,

low-lying electronic excitations) may also be studied with thermal neutrons. The basic experiment is a scattering experiment, in which a neutron of wavevector $\boldsymbol{k}_{\mathrm{i}}$ and energy $E(\boldsymbol{k}_{\mathrm{i}})$ scatters inelastically off the crystal, to create a quantum of vibration with energy $\hbar\boldsymbol{k}_j(\boldsymbol{Q})$. Since wavevectors are conserved, the wavevector of the scattered neutron is

$$\boldsymbol{k}_{\mathrm{s}} = \boldsymbol{k}_{\mathrm{i}} \pm \boldsymbol{Q}, \tag{1.1}$$

where the upper sign is used if a phonon is absorbed in the scattering process (phonons are present by virtue of the finite temperature of the crystal), and the lower sign is used if a phonon is created. Similarly, energy is conserved, so

$$E(\boldsymbol{k}_{\mathrm{s}}) = E(\boldsymbol{k}_{\mathrm{i}}) \pm \hbar\omega_j(\boldsymbol{Q}). \tag{1.2}$$

The vibrational spectroscopy of surfaces may be discussed along lines very similar to those for crystals, if the surface is viewed as a two-dimensional lattice. The vibrational normal modes are now characterized by a wavevector $\boldsymbol{Q}_{\parallel}$ parallel to the surface, which lies within the appropriate two-dimensional Brillouin zone (see ch. 5 of Ibach & Mills 1982). In a scattering or absorption event, after assuming perfect crystalline order in the plane parallel to the surface, components of wavevector parallel to the surface are conserved, as is the total energy. But the lack of translational invariance normal to the surface leads to a breakdown of wavevector conservation in this dimension.

It follows that, just as in bulk crystals, the infrared and optical spectroscopies can probe only the region close to the centre of the two-dimensional Brillouin zone, in the optical spectroscopy of clean surfaces or those covered by ordered adsorbate layers. We seek a short-wavelength probe that has the potential of exploring the full two-dimensional Brillouin zone, as thermal neutrons do for bulk crystals.

The discussion of surface vibrational spectroscopy is complicated by one other difficulty. This is that the region under study is only one monolayer of atoms in thickness. The ideal probe is one that samples only the outermost few atomic layers at most. Thermal neutrons have long mean free paths in matter, and as a consequence are not suitable for surface studies, except under limited conditions where the surface:volume ratio is very high and adsorbates present have large cross sections, or perhaps when employed at grazing incidence (Felcher 1981), a possibility yet to be realized in the laboratory in inelastic spectroscopy.

In the past few years, two probes have been used to study surface phonons on clean and adsorbate-covered surfaces. One is the inelastic scattering of monoenergetic, highly collimated beams of neutral He atoms, and the second the inelastic scattering of electrons from the surface. In the first method, the incident He beam typically has a kinetic energy of a few tens of millielectronvolts; the impact energies are thus in the same range as the thermal neutrons employed in studies of bulk phonons (see Toennies 1984). While thermal neutrons penetrate deeply into the solid, as remarked above, the He atoms are reflected back after sampling only the very outermost layer of atoms or adsorbates. In the inelastic scattering event, they sample only the thermal motions in this very outermost layer. Theoretical analysis shows, as expected from elementary kinematic arguments, that it is the thermal motions normal to the surface that provide the dominant contribution to the excitation cross section here (Bortolani *et al.* 1983).

We shall appreciate that to explore the dispersion relations of surface phonons throughout the two-dimensional Brillouin zone with electrons as the probe, it is desirable to employ electron beams with impact energies in the range 100–300 eV. It is then a very demanding task for the

experimentalists to produce such beams sufficiently monoenergetic for the very small losses (5–100 meV) associated with excitation of surface phonons to be detected. Electron beams of this degree of monochromicity have been generated by Ibach and his colleagues, and these have been used to study surface phonons (and surface resonance modes ('leaky surface phonons')) on clean and adsorbate-covered surfaces. Their work is reported in this symposium.

We, together with our colleagues, have pursued a theoretical programme aimed at the development of lattice dynamical models, which may be used to interpret the inelastic electron scattering data, and we have also made extensive studies of the angle and energy variation of the energy loss cross section for excitation of surface phonons by such electron beams. As we shall appreciate, such calculations must make use of an explicit description of the lattice dynamics of the surface, so these two facets of our programme are intertwined. The theory has proved reliable in a fully quantitative sense. Recent data explores the energy variation of the cross section for the excitation of the Rayleigh surface phonon on a clean Ni(100) surface, over a range of impact energies from 50 to 300 eV (Xu *et al.* 1985). The theory provides an excellent account of the complex energy variation found in the experiments. In the original study of surface phonons on the Ni(100) surface by the inelastic electron scattering method (Lehwald *et al.* 1983), only the Rayleigh surface phonon was observed, while surface lattice dynamics predicts that another mode with displacements parallel to the surface should be excited in this scattering geometry. This mode is referred to as the S_6 mode (see ch. 5 in Ibach & Mills 1982). The theory predicts, in the energy range outlined above, that by virtue of multiple scattering resonances the cross section for excitation of S_6 should rise to values comparable to those found for the Rayleigh mode within certain narrow 'energy windows'; subsequent experiments by Ibach and collaborators have verified the theoretical prediction, and found the S_6 mode is indeed excited within the energy windows that emerge from the theory (Xu *et al.* 1985).

This paper is devoted to a discussion of the theory of excitations of surface phonons in inelastic electron scattering, with emphasis on recent calculations. Section 2 is devoted to general remarks that provide an overview of the phenomenon, including a discussion of selection rules operable in inelastic electron spectroscopy. Section 3 then discusses the formalism that is used in the calculations, and §4 examines a number of recent results that shed light on general aspects of the phenomenon.

2. General remarks

The basic experiment of interest is illustrated in figure 1. We imagine that a monoenergetic electron beam with impact energy $E^{(i)}$ and wavevector $\boldsymbol{k}^{(i)}$ strikes the surface. The electron may scatter elastically (diffract) from the crystal, to form the Bragg beams explored in the study of low-energy electron diffraction.

However, as it strikes the surface, it may also sample the thermal vibrations, and create or absorb a vibrational quantum. Such inelastically scattered electrons emerge in between the specular and Bragg beams, by virtue of the momentum transfer associated with excitation or absorption of the phonon. In figure 1, we illustrate an electron deflected away from the specular beam by an amount $\Delta\theta$. There are two conservation laws that control the direction of the emerging beam. The first, familiar from electron–phonon scattering in the bulk of crystals, is conservation of wavevector. If the subscript parallel symbol denotes the projection of a vector onto the plane parallel to the surface, the process of scattering from the two-dimensional surface

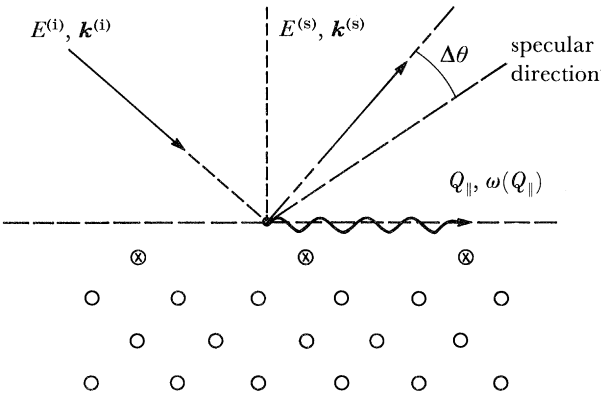

FIGURE 1. The inelastic electron-scattering experiment of central interest to this paper. Electrons of energy $E^{(i)}$ strike the crystal, and a certain fraction create (or absorb) a phonon as they scatter off the surface. They thus emerge with shifted energy, in directions distinct from those where the specular or Bragg beams emerge.

leads to the conservation of components of wavevector within the surface, to within a reciprocal lattice vector $\boldsymbol{G}_\parallel$ of the surface region, here assumed perfectly periodic. Thus if $\boldsymbol{k}_\parallel^{(s)}$ and $\boldsymbol{k}_\parallel^{(i)}$ are suitable projections of the wavevector of the scattered and incident electron, and if $\boldsymbol{Q}_\parallel$ is the wavevector of the phonon created in the scattering event, then

$$\boldsymbol{k}_\parallel^{(s)} = \boldsymbol{k}_\parallel^{(i)} \pm \boldsymbol{Q}_\parallel + \boldsymbol{G}_\parallel, \tag{2.1}$$

with the choice of sign dictated by where the phonon is created (plus sign) or absorbed (minus sign) in the scattering event. Conservation of energy dictates that, if $E^{(s)}$ is the energy of the scattered electron,

$$E^{(s)} = E^{(i)} \pm \hbar\omega(\boldsymbol{Q}_\parallel). \tag{2.2}$$

Given the direction and energy of an electron scattered off the surface after phonon creation or absorption, from (2.1) and (2.2), one may deduce the wavevector and frequency of the phonon responsible for the scattering event. Associated with a given wavevector $\boldsymbol{Q}_\parallel$, there is the possibility of several distinct branches of surface phonons, each of which may scatter the electrons (Wallis 1973). Furthermore, as pointed out in an early discussion of off-specular scattering of electrons by phonons, bulk phonons that propagate up to the surface and scatter off it may also produce loss features in the spectrum (Roundy & Mills 1972). More recently, it is clear that long-lived surface resonances may be present as a consequence of resonant excitation of the surface region by the bulk phonons; these produce features in the experimental loss cross section very similar to those from true surface phonons (Rahman *et al.* 1983*a*, *b*).

Thus, associated with a given wavevector transfer $\boldsymbol{Q}_\parallel$, there are several distinctly different loss features in general. One simplification in the data analyses is that to very good approximation, in electron energy loss spectroscopy, *all* excitations characterized by a particular wavevector $\boldsymbol{Q}_\parallel$ scatter electrons into the same *direction*; a scan of the loss spectrum associated with a given *direction* of emergence from the surface thus provides information on the frequencies of modes associated with a given *wavevector* $\boldsymbol{Q}_\parallel$ (Roundy & Mills 1972). That this is so follows upon noting that to calculate the direction of the emerging scattered beam, one may ignore the factor of $\hbar\omega(\boldsymbol{Q}_\parallel)$ in (2.2). The energy of the incident and scattered electron will be tens of electronvolts, while $\hbar\omega(\boldsymbol{Q}_\parallel)$ is of the order of 100 meV or less.

So, the direction into which the electron is scattered is controlled by the *wavevector* of the phonon responsible for the scattering event, but is insensitive to its *frequency*. This feature of electron energy loss spectroscopy renders direct comparison between the data and theory very easy, since the theorist typically directly calculates the spectral densities at fixed wavevector, which is precisely what is measured here (see, for example, Rahman *et al.* 1984). In the inelastic He scattering experiments, the energies of the incident and scattered atoms are quite comparable to those of the vibrational quanta. Thus, when one measures the loss spectrum at a given *scattering angle*, one samples a *range* of wavevectors $\boldsymbol{Q}_{\parallel}$ parallel to the surface. Direct comparison between theory and experiment thus requires a greater expenditure of labour.

When one scans the angular distribution of electrons scattered inelastically from the surface, a characteristic feature is the appearance of an intense lobe of electrons that suffer small-angle deflections. If ω_0 is the frequency of the mode responsible for the scattering, then theoretical considerations show that the near-specular lobe is confined to angular deflections $\Delta\theta$ (figure (1)) of the order of $\Delta\theta_E = \hbar\omega_0/2E^{(\mathrm{i})}$, where $E^{(\mathrm{i})}$ is the energy of the incident beam (see ch. 3 of Ibach & Mills 1982). The physical origin of the intense small-angle scattering is by now well understood, and may be described in quantitative terms by theory (Ibach & Mills 1982.) As an atom on or in the crystal surface vibrates, the low symmetry of the surface environment leads to a time-dependent electric dipole moment; as the bond lengths are modulated by the vibration, charge is transferred onto and off the atom, with a period equal to that of the vibration. This time-dependent dipole moment generates an oscillatory electric field in the vacuum above the crystal; as the electron approaches the surface, it scatters inelastically from these electric-field fluctuations.

It is the long-ranged nature of the electric dipole field that is responsible for the peak in the scattering cross section at small momentum transfer. An elementary agreement suffices to see how this comes about. Let $\phi(\boldsymbol{x}_{\parallel}, z)\exp(-\mathrm{i}\omega_0 t)$ be the electrostatic potential encountered by the electron as it approaches the surface. Here, z is the coordinate of the electron normal to the surface, and $\boldsymbol{x}_{\parallel}$ that parallel to the surface plane. A wave-like normal mode with wavevector $\boldsymbol{Q}_{\parallel}$ parallel to the surface then must produce a potential in the vacuum above the crystal of the form $\phi(\boldsymbol{x}_{\parallel} z) = \boldsymbol{\Phi}(z)\exp(\mathrm{i}\boldsymbol{Q}_{\parallel}\cdot\boldsymbol{x}_{\parallel})$. This potential must necessarily satisfy Laplace's equation, and it is a very short exercise to see that one must have $\boldsymbol{\Phi}(z) \sim \exp(-Q_{\parallel} z)$. Long-wavelength modes (those with small values of $\boldsymbol{Q}_{\parallel}$) thus lead to very long-ranged fields in the vacuum. From the kinematical relations in (2.1) and (2.2), it follows that such long-wavelength modes lead to small-angle deflections.

Nearly all early inelastic electron-scattering studies of surface vibrations confine their attention to the near-specular lobe just described, where the signal is particularly strong. In this angular régime, a selection rule proposed a number of years ago (Evans & Mills 1972) operates in this angular region. The selection rule states that the only vibrational normal modes that contribute to the near-specular lobe are those that generate an oscillatory electric dipole moment normal to the surface. This selection rule is in fact identical to that invoked to interpret studies of surface vibrations by the method of infrared spectroscopy (Greenler 1966, 1969). Electron energy loss spectroscopy has had a major impact on surface vibrational spectroscopy because of its great spectral range. In one measurement with an instrument of very high resolution (2 meV, or 16 cm^{-1}), one may scan continuously from below 100 cm^{-1}, to as large a loss as one wishes.

From the remarks above, it follows that the normal modes excited by those inelastically

scattered electrons that contribute to the dipole lobe have wavevectors $\boldsymbol{Q}_{\parallel}$ of the order of $k^{(i)}\Delta\theta_E$, where $k^{(i)}$ is the wavevector of the incident electron. For technical reasons, impact energies in these experiments are typically about 5 eV, so $k^{(i)} \sim 10^8$ cm^{-1}. If we consider excitation of a vibrational quantum with energy to $\hbar\omega_0 \sim 50$ meV, then $\Delta\theta_E \sim 0.3°$ (below the angular resolution of current spectrometers), and $Q_{\parallel} \sim 5 \times 10^5$ cm^{-1}. In the language of solid state physics, where the dispersion curves of phonons throughout the two-dimensional Brillouin zone are of interest, at the Brillouin zone boundary one has $Q_{\parallel} \sim 10$ cm^{-1}. Thus, near-specular electron energy loss spectroscopy can only explore the region very near the centre of the two-dimensional Brillouin zone.

If we wish to use electron energy loss spectroscopy to explore the *entire* two-dimensional Brillouin zone, and pursue the analogy with neutron scattering from bulk crystals outlined earlier in the present paper, quite clearly we must examine electrons that suffer large-angle deflections in the inelastic scattering event. These emerge far outside the near-specular lobe, where the scattering intensity is very weak. Electrons that suffer such large-angle deflections are clearly present; they constitute the thermal diffuse background present in low-energy diffraction studies of high-quality single-crystal surfaces. Many years ago, a discussion explored the information contained in the energy spectrum of those electrons that contribute to the thermal diffuse background; through its study one may deduce the dispersion relations of surface phonons with wavelengths comparable to the lattice constant, and these along with other features in the loss cross section are sensitive to microscopic aspects of surface lattice dynamics (Roundy & Mills 1972).

From the remarks above, the theoretical ingredients that must be incorporated into a description of large-angle, inelastic scattering of electrons from surface phonons are evident. If we consider excitation of a surface phonon with large wavevector, $Q_{\parallel} \approx 10^8$ cm^{-1}, then long-ranged contributions to the electron–surface interaction such as those producing the near-specular lobe are quite unimportant. The electrostatic potential, proportional to $\exp(-Q_{\parallel} z)$ in the vacuum, has decayed to zero within one ångström of the surface. Furthermore, for electrons in the 10–300 eV kinetic energy range, we know that the incoming electron samples three or four atomic layers after it strikes the surface. Thus, rather than focus attention on the electric-field fluctuations in the vacuum above the crystal the electron samples as it approaches the surface, our primary concern is its interaction with the crystal potential *after* it enters the crystal.

We have developed a formalism that describes excitation of surface phonons by a low-energy electron, under the conditions outlined in the previous paragraph (Tong *et al.* 1980; Li *et al.* 1980). This theory has now been implemented and applied to the analysis of several adsorbate–substrate complexes, so trends in the energy and angle variation of the excitation cross section have been explored quite thoroughly. We find a series of selection rules, some group theoretic in origin and some approximate in nature, apply in the large-angle deflection régime (Tong *et al.* 1981).

The theory has recently achieved a remarkable success in our view: in advance of experiment, it predicted narrow-energy windows in the range 50–300 eV, within which multiple scattering resonances greatly enhance the cross section for the S_6 surface phonon in the Ni(100) surface. This is a mode, which at the two dimensional Brillouin zone boundary, involves atomic motions strictly parallel to the surface in the outermost atomic layer (see ch. 5 in Ibach & Mills 1982). It follows that kinematical estimates show the excitation cross section to be very small compared

to that of the S_4 (Rayleigh) surface phonon, which is polarized normal to the surface in the outermost atomic layer; only the S_4 mode is as observed in the first study of surface phonons by the method of electron energy loss spectroscopy (Lehwald *et al.* 1983). Subsequent to the theoretical prediction of enhancement of the S_6 cross section by multiple scattering resonances, this mode is as observed within, and only within, the three energy windows predicted by theory. The same series of calculations explore the energy variation of the cross section for excitation of the S_4 Rayleigh surface phonon in the 50–300 eV range, to achieve remarkable agreement with new experimental data. A recent publication describes the new experiment and comparison between theory and experiment (Xu *et al.* 1985).

The remainder of this paper is devoted to a summary of the formalism used in the above calculations, and a summary of the theoretical results.

3. The theory of large-angle inelastic electron scattering

A formalism within which one may calculate the cross section for the scattering of low-energy electrons from crystal surfaces has been developed by the present authors (Li *et al.* 1980). The theory takes full account of penetration of the electron into the crystal, and the subsequent multiple scattering from the ion cores as it approaches and exits from the site where excitation of a surface phonon occurs. The formalism is arranged to apply to structures that exhibit periodicity in the two directions parallel to the surface, and thus may be applied to excitation of phonons upon reflection from a perfect surface, or a surface upon which a two-dimensionally periodic array of atoms or molecules is adsorbed. In principle, one may apply the method to analyse imperfect surfaces, though this has yet to be done.

Central to the scheme is the adiabatic approximation; typical atomic vibrational energies are very small, on the scales of energies of the incoming and scattered electrons. We may thus assume the electron encounters and scatters off a disordered lattice, where the disorder has its origin in the thermal motions of the atoms. We may proceed by considering the scattering from a lattice with frozen-in disorder, and then we may average over all possible such disordered configurations.

For simplicity in notation, we consider here scattering from the surface of a perfect monoatomic crystal, though the generalization is very straightforward, and is given in the original paper cited above. Each atom has an instantaneous position given by $\boldsymbol{R}(\boldsymbol{l}_\parallel l_z)$, where $l_\parallel$ is a vector that denotes its equilibrium position in a plane parallel to the surface, l_z units from the surface. We write $\boldsymbol{R}(\boldsymbol{l}_\parallel l_z) = \boldsymbol{R}_0(\boldsymbol{l}_\parallel l_z) + \boldsymbol{u}(\boldsymbol{l}_\parallel l_z)$, with $\boldsymbol{u}$ the amplitude of the thermal motion. We consider $f(\boldsymbol{k}^{(\mathrm{i})}\, \boldsymbol{k}^{(\mathrm{s})}; \{\boldsymbol{R}(\boldsymbol{l}_\parallel l_z)\})$, the scattering amplitude deflecting the electron from its initial direction $\boldsymbol{k}^{(\mathrm{i})}$ to its final direction $\boldsymbol{k}^{(\mathrm{s})}$; here $\boldsymbol{R}(\boldsymbol{l}_\parallel, l_z)$ is the instantaneous position of the atom. Now if the amplitude of thermal vibrations is small, then we may write, with $\boldsymbol{R}_\beta(\boldsymbol{l}_\parallel l_z)$ the βth cartesian component $\boldsymbol{R}(\boldsymbol{l}_\parallel l_z)$,

$$f(\boldsymbol{k}^{(\mathrm{i})}, \boldsymbol{k}^{(\mathrm{s})}; \{\boldsymbol{R}(\boldsymbol{l}_\parallel l_z)\}) = f(\boldsymbol{k}^{(\mathrm{i})}, \boldsymbol{k}^{(\mathrm{s})}; \{R^{(0)}(\boldsymbol{l}_\parallel l_z)\}) + \sum_{l'_\parallel l'_z} \sum_{\alpha} \left(\frac{\partial f}{\partial R_\beta (\boldsymbol{l}'_\parallel l'_z)}\right) \{\boldsymbol{R}^{(0)}_\beta (\boldsymbol{l}_\parallel l_z)\}\, u_\beta(\boldsymbol{l}'_\parallel l'_z) + \ldots . \quad (3.1)$$

The first term in (3.1) describes the scattering of the electron from the perfectly periodic array, with all atoms in their equilibrium positions. This is just the quantity calculated in the theory

of low-energy electron diffraction (for a review, see Tong 1975). As we shall appreciate, the second term describes processes in which a single vibrational quantum is created and destroyed. It is necessary to break this term down into its component parts.

First of all, consider $u_\beta(\boldsymbol{l}_\parallel l_z)$, the amplitude of the vibrational motion of the atoms. If the vibrations are treated in the harmonic approximation of lattice dynamics, then this object may be expressed in terms of the annihilation and creation operators a_s, a_s^+ of the normal modes, along with the eigenvectors $e_\beta^{(s)}(\boldsymbol{l}_\parallel, l_z)$. Here s is a symbol that denotes the set of quantum numbers required to describe the normal modes of the set of masses. If the eigenvectors are normalized so that

$$\sum_{\beta, \boldsymbol{l}_\parallel l_z} |e_\beta^{(s)}(\boldsymbol{l}_\parallel l_z)|^2 = 1, \tag{3.2}$$

we have

$$u_\beta(\boldsymbol{l}_\parallel l_z) = \sum_s \left(\frac{\hbar}{2M\omega_s}\right)^{\frac{1}{2}} e_\beta^{(s)}(\boldsymbol{l}_\parallel l_z)\ (a_s + a_s^+). \tag{3.3}$$

For our perfect crystal, periodic in the two dimensions parallel to the surface, each vibrational normal mode is described by a two-dimensional wavevector parallel to the surface, $\boldsymbol{Q}_\parallel$, which lies in the appropriate two-dimensional Brillouin zone. Thus, the symbol s may be replaced by the combination $(\boldsymbol{Q}_\parallel \alpha)$, where α denotes which normal mode of wavevector $\boldsymbol{Q}_\parallel$ is of concern. This index may refer to a surface phonon, or bulk phonon that propagates up to the surface, and reflects off it. Such modes contribute to the loss cross section also (Roundy & Mills 1972), and produce distinctive features in it due to resonance excitation of the surface in response to the bulk mode (Rahman *et al.* 1983*a*, *b*). Then if we consider a large crystal, with N_s atoms in a basic quantization plane normal to the surface we have

$$e_\beta^{(s)}(\boldsymbol{l}_\parallel l_z) \to e_\beta^{(\boldsymbol{Q}_\parallel \alpha)}(l_z)\ N_s^{-\frac{1}{2}} \exp\{i\boldsymbol{Q}_\parallel \cdot \boldsymbol{R}_0(\boldsymbol{l}_\parallel, l_z)\}, \tag{3.4}$$

where $e_\beta^{(\boldsymbol{Q}_\parallel \alpha)}(l_z)$ is now normalized so that

$$\sum_{l_z} |e_\beta^{(\boldsymbol{Q}_\parallel \alpha)}(l_z)|^2 = 1. \tag{3.5}$$

Then the scattering amplitude $\delta f_{\boldsymbol{Q}_\parallel \beta}(\boldsymbol{k}^{(i)}, \boldsymbol{k}^{(s)})$ associated with excitation of the particular normal mode $(\boldsymbol{Q}_\parallel \alpha)$ may be written

$$\delta f_{\boldsymbol{Q}_\parallel \alpha}(\boldsymbol{k}^{(i)}, \boldsymbol{k}^{(s)}) = \left(\frac{\hbar}{2MN_s\omega(\boldsymbol{Q}_\parallel \alpha)}\right)^{\frac{1}{2}} [a_{\boldsymbol{Q}_\parallel \alpha} + a^+_{-\boldsymbol{Q}_\parallel \alpha}] \times \sum_{\beta l_z} e_\beta^{(\boldsymbol{Q}_\parallel \alpha)}(l_z) \sum_{\boldsymbol{l}_\parallel} \left(\frac{\partial f}{\partial R_\beta(\boldsymbol{l}_\parallel l_z)}\right) \exp\{i\boldsymbol{Q}_\parallel \cdot R_0(\boldsymbol{l}_\parallel l_z)\}. \tag{3.6}$$

We turn our attention next to the calculation of the scattering amplitude derivative $(\partial f/\partial R_\beta)$, which appears in (3.6). A particularly complete discussion of the formalism used for this purpose has been given by Hall (1983). The discussion presented here follows that given by him.

What we wish to calculate is the amplitude for scattering from a state $\boldsymbol{k}^{(i)}$ in the vacuum *above* the crystal, to a final state $\boldsymbol{k}_<^{(s)}$ also *above* the crystal. We begin by assuming that both the incident and final beam are simply refracted at the crystal–vacuum interface, as illustrated in figure 2*b*. The calculation we then pursue is that of calculating the amplitude for scattering from a state $\boldsymbol{k}^{(i)}$ just *inside* the crystal, to a final state $\boldsymbol{k}_>^{(s)}$ just *inside* the crystal. After discussing the formal structure of this calculation, as it has been executed in the recent work, we then

turn to the question of relating this to the desired scattering amplitude, for scattering from $\boldsymbol{k}_{>}^{(\mathrm{i})}$ to $\boldsymbol{k}_{>}^{(\mathrm{s})}$. We shall appreciate the motivation for making this separation shortly.

If we consider the disordered crystal depicted in figure 2*a*, and let

$$V = \sum_{l_\parallel l_z} v(\boldsymbol{r} - \boldsymbol{R}(\boldsymbol{l}_\parallel l_z)) \tag{3.7}$$

be the crystal potential encountered by the electron wave, then the scattering amplitude $f(\boldsymbol{k}_{<}^{(\mathrm{i})}, \boldsymbol{k}_{<}^{(\mathrm{s})}; \{\boldsymbol{R}(\boldsymbol{l}_\parallel l_z)\})$ may be written, from scattering theory,

$$f(\boldsymbol{k}_{<}^{(\mathrm{i})}, \boldsymbol{k}_{<}^{(\mathrm{s})}; \{\boldsymbol{R}\}) = \langle \boldsymbol{k}_{<}^{(\mathrm{s})} | GT | \boldsymbol{k}_{<}^{(\mathrm{i})} \rangle; \tag{3.8}$$

here $|\boldsymbol{k}_{<}^{(\mathrm{i,s})}\rangle$ describes the plane wave incident and final states inside the crystal, G is the electron propagator in the 'average crystal', i.e. a medium with constant (optical) potential that represents the inner potential of the crystal. The quantity T is the T matrix of scattering theory, defined as below. Here and elsewhere, integrations over appropriate coordinates are assumed. Thus

$$\langle \boldsymbol{k}_{<}^{(\mathrm{s})} | GT | \boldsymbol{k}_{<}^{(\mathrm{i})} \rangle = \int \mathrm{d}^3 r_1 \, \mathrm{d}^3 r_2 \, \mathrm{d}^3 r_3 \exp\{-\mathrm{i}\boldsymbol{k}_{<}^{(\mathrm{s})} \cdot \boldsymbol{r}_1\} G(\boldsymbol{r}_1 - \boldsymbol{r}_2) \, T(\boldsymbol{r}_2, \boldsymbol{r}_3) \exp\{\mathrm{i}\boldsymbol{k}_{<}^{(\mathrm{i})} \cdot \boldsymbol{r}_3\}. \tag{3.9}$$

Several assumptions are implicit in the above relations. First of all, (3.7) assumes that when an ion is displaced from its equilibrium position, by virtue of the thermal motion, the potential

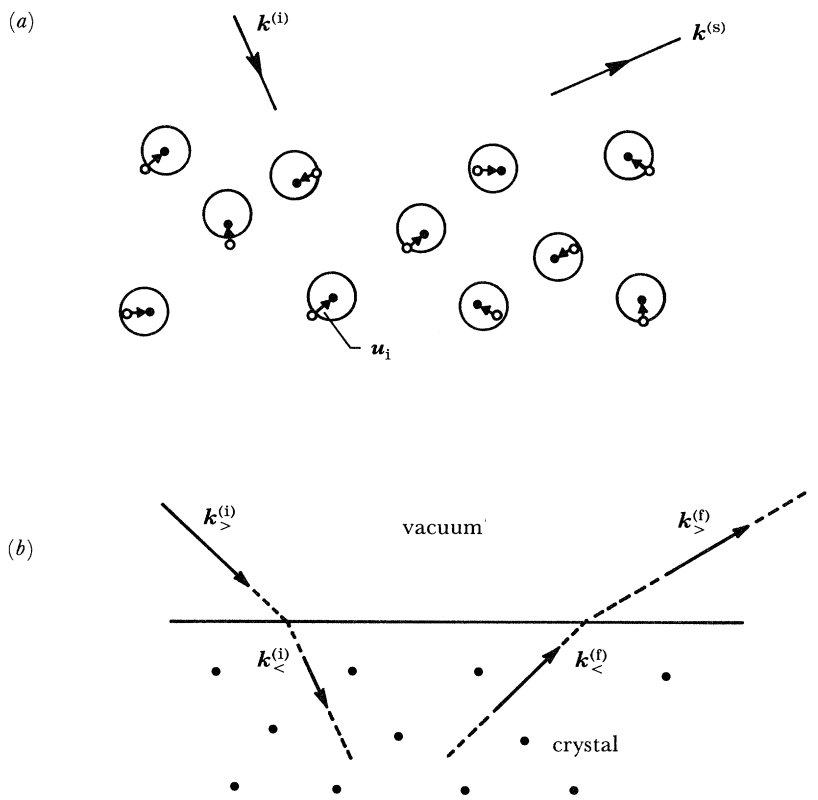

FIGURE 2. (*a*) A crystal that contains disorder by virtue of the thermal motions of the atoms in it. The open circles are the equilibrium positions of the atom, and the solid dots the instantaneous position of the nuclei. (*b*) The theory calculates the amplitude for scattering from state $\boldsymbol{k}_{>}^{(\mathrm{i})}$ in the vacuum above the crystal, to state $\boldsymbol{k}_{>}^{(\mathrm{f})}$ in the vacuum above. One proceeds first by calculating the amplitude for scattering from $\boldsymbol{k}_{<}^{(\mathrm{i})}$ inside, to state $\boldsymbol{k}_{<}^{(\mathrm{f})}$ inside, as discussed in the text.

that surrounds its nucleus is *rigidly* displaced, unchanged in form. In the calculations we have made to date, this is chosen to be a spherically symmetric muffin-tin potential. As we shall see, this assumption allows us to express all quantities that enter the calculation in terms of the phase shifts for elastic scattering of the ions in the crystal.

In (3.8), only T depends on the positions of the ions, so that

$$\frac{\partial f}{\partial R_\beta(\boldsymbol{l}_\parallel l_z)} = \left\langle \boldsymbol{k}_<^{(\mathrm{s})} \left| G \frac{\partial T}{\partial R_\beta(\boldsymbol{l}_\parallel l_z)} \right| \boldsymbol{k}_<^{(\mathrm{i})} \right\rangle. \tag{3.10}$$

Now the T matrix for the disordered crystal satisfies, again with spatial integrations implicit,

$$T = V + VGT, \tag{3.11}$$

or upon iterating,

$$T = V + VGV + VGVGV + \ldots. \tag{3.12}$$

Upon differentiating and rearranging the series, one sees easily that

$$\frac{\partial T}{\partial R_\beta(\boldsymbol{l}_\parallel l_z)} = (1 + T_0 G) \frac{\partial V}{\partial R_\beta(\boldsymbol{l}_\parallel l_z)} (1 + G T_0), \tag{3.13}$$

where T_0 is the T matrix for scattering off the *perfect* crystal, in which all ions reside on their proper lattice sites. Then

$$\frac{\partial f}{\partial R_\beta(\boldsymbol{l}_\parallel l_z)} = \left\langle \boldsymbol{k}_<^{(\mathrm{s})} \left| (G + G T_0 G) \left(\frac{\partial V}{\partial R_\beta(\boldsymbol{l}_\parallel l_z)} \right) (1 + G T_0) \right| \boldsymbol{k}_<^{(\mathrm{i})} \right\rangle. \tag{3.14}$$

The state vector $(1 + G T_0)|\boldsymbol{k}_<^{(\mathrm{i})}\rangle$ is simply the state vector generated in a low-energy electron diffraction (l.e.e.d.) calculation. It thus has the Bloch property, with respect to translations parallel to the surface. Let us choose a particular unit cell in plane l_z designated as the cell with $\boldsymbol{l}_\parallel = 0$. Then if the l.e.e.d. wavefunction is evaluated at any point within this special unit cell, and its value compared to that at the equivalent point in unit cell $(\boldsymbol{l}_\parallel l_z)$, the two differ by simply the phase factor $\exp\{\mathrm{i}\boldsymbol{k}_<^{(\mathrm{i})} \cdot \boldsymbol{R}_0(\boldsymbol{l}_\parallel l_z)\}$. A similar argument applies to the final state vector in (3.14). We may then relate $(\partial f / \partial R_\beta(\boldsymbol{l}_\parallel l_z))$ for any cell in lattice plane l_z, to that in the reference cell at $\boldsymbol{l}_\parallel = 0$ by a simple rule:

$$\left(\frac{\partial f}{\partial R_\beta(\boldsymbol{l}_\parallel l_z)} \right) = \exp\{\mathrm{i}(\boldsymbol{k}_<^{(\mathrm{i})} - \boldsymbol{k}_<^{(\mathrm{s})}) \cdot \boldsymbol{R}_0(\boldsymbol{l}_\parallel l_z)\} \left(\frac{\partial f}{\partial R_\beta(0, l_z)} \right)_0. \tag{3.15}$$

This relation allows one to make the sum over $\boldsymbol{l}_\parallel$ in (3.6), to find, with $\{\boldsymbol{G}_\parallel\}$ the set of reciprocal lattice vectors that characterize the two-dimensionally periodic crystal,

$$\delta f_{\boldsymbol{Q}_\parallel \alpha}(\boldsymbol{k}_<^{(\mathrm{i})}, \boldsymbol{k}_<^{(\mathrm{s})}) = (\hbar N_\mathrm{s} / 2M\omega(\boldsymbol{Q}_\parallel \alpha))^{\frac{1}{2}} [a_{\boldsymbol{Q}_\parallel \alpha} + a^+_{+\boldsymbol{Q}_\parallel \alpha}] \{ \sum_{\boldsymbol{G}_\parallel} \delta_{\boldsymbol{k}_<^{(\mathrm{s})}; \boldsymbol{k}_<^{(\mathrm{i})} + \boldsymbol{Q}_\parallel + \boldsymbol{G}_\parallel} \}$$
$$\times \sum_{\beta l l'} e_\beta^{\boldsymbol{Q}_\parallel \alpha}(l_z) \left\{ \frac{\partial f}{\partial R_\beta(0, l_z)} \right\}. \tag{3.16}$$

The wavevector conservation law discussed in (2.1) is contained in (3.16). In this regard, note that parallel components of electron wavevector are all conserved as the electron emerges from within the crystal into the vacuum (figure 2*b*).

Elsewhere we have presented a discussion of how to pass from (3.16) to an expression for

the excitation cross section, for scattering off the mode $(\boldsymbol{Q}_{\parallel}\alpha)$. (Li *et al.* 1980). There we also provide a detailed prescription for calculating $(\partial f/\partial R_\beta(0, l_z))$, in terms of the propagation matrices that enter the theory of low-energy electron diffraction (Tong 1975). There is one new element that enters the present calculation: one requires the matrix element of $(\partial v/\partial R_\beta)$ between the electron states of interest. Within the spherically symmetric muffin-tin model, this may be reduced to the evaluation of radial integrals of the form

$$I^{\pm} = \int_0^{R_0} \mathrm{d}r\, r^2 R_{l\pm1}(r)\, (\mathrm{d}v(r)/\mathrm{d}r) R_l(r), \tag{3.17}$$

where R_0 is the muffin-tin radius, and $R_e(r)$ is the radial portion of the solution of Schrödinger's equation within the reference cell, where the muffin-tin potential $v(r)$ had been displaced. These integrals may be expressed in terms of the phase shifts for elastic scattering off the potential (see footnote 5 of Gaspari & Gyorffy 1972).

The ingredients of the cross section calculation are now clear. We choose a reference cell in each layer of the crystal, then calculate the scattering amplitude derivatives $(\partial f/\partial R_\beta(0, l))$ for each layer. If we suppose, for the purpose of the discussion, that we know the geometrical structure of the surface, then within the theoretical picture outlined above, we need *no new theoretical input* beyond that required for a l.e.e.d. calculation (though the numerical calculations involved are substantially more time consuming!). We then form the *total* amplitude for phonon excitation by coherently superimposing the amplitude derivatives for various layers, as described by (3.16).

To do this, at least in principle, we face a 'chicken and egg' question. To calculate the cross section for exciting any particular surface phonon, to form the coherent superposition of the derivatives $(\partial f/\partial R_\beta(0, l_z))$, we require the eigenvector $\boldsymbol{e}^{(\boldsymbol{Q}_{\parallel}\alpha)}(l_z)$ of the mode of interest. This can be generated by the theory of surface lattice dynamics, but to proceed one requires knowledge of the interatomic force constants near the crystal surface. One may begin an analysis by modelling the bulk phonon spectrum of the crystal, and then assuming that the force constants near the surface are unchanged from their bulk values. This may be a highly unrealistic assumption. In general, surface relaxation can lead to substantial changes in interatomic force constants. A change of an interatomic bond length of just a small percentage can result in a force constant change of 20–30%; the nature of the eigenvectors near the surface (and, of course, also the frequency of the mode) are influenced substantially by such a change. Note that even in the absence of bond length changes induced by surface relaxation, the electronic structure of atoms near the surface may differ from those in the bulk, and this is another source of force-constant changes. Our own earlier work on the surface phonons on a clean Ni(100) surface establishes that the force constant that couples the atoms in the outermost layer to those in the first interior layer of the crystal is larger than the bulk value by 20% (Lehwald *et al.* 1983). An inward contraction of 3% between the outermost atomic layers is a likely source of this change. When the same surface is covered by the $c(2\times2)$ overlayer of oxygen, there is a 5% *outward* relaxation of this layer (Frenken *et al.* 1983), and we find a dramatic *softening* of the force constant, upon analysing the dispersion curves of the S_4 surface phonon on the adsorbate-covered surface (Szeftel *et al.* 1983). A systematic discussion of the influence of the $c(2\times2)$ overlayers of sulphur, oxygen, and carbon on surface force constants of Ni(100) has been given recently (Rahman & Ibach 1985).

So to calculate cross sections reliably for excitation of surface phonons, one requires

information on the atomic force constants, in principle. This requires information in advance on the nature of the phonons themselves, so we are trapped if we wish to make predictive calculations in advance of information on the nature of the dispersion curves. Extensive calculations have been made, which explore this issue, and the situation is not as bad as just outlined. First, if one considers internal vibration modes of adsorbed molecules, or those of light atoms, the frequencies of the modes in question lie well above the phonon frequencies of the substrate. Then to an excellent approximation, the substrate atoms may be assumed at rest, and in this limit reliable pictures of the eigenvectors are readily generated by simple models. Our analysis of off-specular scattering from adsorbed CO molecules provides an example (Tong *et al.* 1981).

Recently, with our collaborators, one of us has made extensive studies of the energy variation of the cross sections for exciting two surface phonons on the clean Ni(100) surface, the S_4 and the S_6 mode (Xu *et al.* 1985). The S_4 mode, whose dispersion curve had been measured earlier on the Ni(100) surface (Lehwald *et al.* 1983) is the mode that evolves into the Rayleigh surface phonon of elasticity theory in the long wavelength limit. At the $\overline{X}$ point of the Brillouin zone, the atomic displacements in the surface are normal to the surface; the *pattern* of atomic displacements is totally determined by this fact, and the wavevector of the mode (a simple discussion of the surface phonons on Ni(100) is given in ch. 5 of Ibach & Mills 1982). The calculations show that the dominant contribution (over 90%) to the cross section for exciting S_4 at $\overline{X}$ comes from the atomic displacements in the *outermost* layer; the surface phonon has a displacement field that has appreciable amplitude in the outermost two or three layers. But the displacement amplitude in the second layer is considerably smaller than in the outermost layer, and at the same time the electron wave is attenuated appreciably by the time it reaches the second layer. After scattering off a displaced second-layer atom, it is attenuated once again as it exists from the crystal. The cross section thus receives its dominant contribution from the term in the sum over l_z in (3.16), which refers only to the outermost layer.

A similar statement can be made about the S_6 mode for suitable scattering geometries. Once again, at $\overline{X}$, the displacement pattern is entirely determined by symmetry in the outer layer. The displacements are now parallel to the surface, and to the wavevector of the mode, in the outermost layer. The series of calculations show once again that the dominant contribution comes from their term in (3.16), which refers to the outermost layer, in scattering geometries realized in the laboratory (Xu *et al.* 1985). We present these calculations in §4.

So, if we concentrate on calculating the cross section for exciting surface phonons at special points of the two-dimensional Brillouin zone, simple considerations yield the nature of the atomic displacements in the outermost surface layer. If we then assume that the dominant contribution to the cross section comes from the vibrational motion of the atoms in the outermost atomic layer, and conditions for this are outlined in §4, then we can make predictive calculations of the surface-phonon excitation cross sections *without* detailed knowledge of the surface force constants. We are left with only an energy- and angle-independent multiplicative prefactor (the actual amplitude of the atomic motion in the outermost layer, combined with factors that contain the frequency of the mode, unknown in advance of measurement.)

If the programme outlined is completed, then we have the amplitude for scattering from a state $\boldsymbol{k}_<^{(i)}$ *inside* the crystal, to the final state $\boldsymbol{k}_<^{(f)}$ *inside* the crystal, as illustrated in figure 2*b*. Of course, of experimental interest is the cross section for scattering from a state $\boldsymbol{k}_>^{(i)}$ *outside* the crystal, to a final state $\boldsymbol{k}_>^{(f)}$ *outside* the crystal. The next question that arises is how one constructs the amplitude just described to that for scattering outside the crystal.

PHILOSOPHICAL TRANSACTIONS OF THE ROYAL SOCIETY A MATHEMATICAL, PHYSICAL & ENGINEERING SCIENCES

From knowledge of the scattering amplitude just described, in essence we have in hand complete information on those Bloch states *inside* the crystal that satisfy boundary conditions appropriate to the scattering problem of interest (Tong 1975). If we take the potential experienced outside the crystal to be a constant, with a step discontinuity at the crystal interface, then it is straightforward to derive boundary conditions that ensure continuity of the wavefunction outside the crystal, along with its derivative normal to the interface. We may then link the 'inside' scattering amplitude to that between states outside the crystal in a straightforward manner.

Unfortunately, this procedure fails to suffice for a number of electron energy loss experiments. It is common practice to employ rather modest beam energies in the experiments, in the range 1–10 eV. As such very slow electrons approach or exit from the crystal, their motion is influenced very importantly by the image potential. Thus, rather than match plane waves in the vacuum to the 'inside' solutions, we must employ basis states that incorporate the influence of the image potential.

Far from the surface, the image potential contribution to the electron–surface interaction has the simple form $-e^2/4z$, with z the distance of the electron from the surface. If this form were applicable for *all* values of z, then the electron eigenwaves are Whittaker functions, and the matching procedure can be readily extended to this case. However, when the electron is close to the surface, within one or two Ångstroms from it, it is well established theoretically that the effective image potential deviates from the simple classical form. In effect, the effective image potential must 'round off', to join smoothly onto the inner potential of the crystal, as the electron enters the crystal surface. We have made an extensive series of calculations of the angle and energy variation of the cross section for large-angle inelastic scattering of electrons from the vibrational motions of the hydrogen adsorbed on the W(100) surface. (Hall *et al.* 1983). These calculations were aimed at providing a quantitative account of both l.e.e.d. data on the W(100) and W(110) surfaces, which is influenced dramatically by the image potential at low impact energies (Adnot & Carette 1977; Baribeau & Carette 1981*a*, *b*), and also the angular profile of the cross sections for excitations of the vibrations of the hydrogen adsorbate, parallel to the surface. Such data were reported by Willis and collaborators, in the first off-specular studies of surface vibrations by the electron energy loss method (Ho *et al.* 1978, 1980; Willis 1979). The experiments were made at an impact energy of 5.5 eV, and our calculations illustrate that the calculated angular profiles are influenced very strongly by the precise manner in which the image potential is rounded off, and joined to the inner potential. While we were successful in accounting for both the l.e.e.d. and energy loss data with a single phenomenological form for the image potential, a very considerable expenditure of computational labour was expended in the process.

The attempt to bring theory and experiment into quantitative contact, and to use the theory as a guide to experiment, is then very complicated if the electron impact energies are sufficiently low that the motion of the incoming and scattered electrons is influenced strongly by the image potential. A whole new element enters the theoretical analysis, and we have little quantitative theory to guide us.

The original experiments of Ibach and collaborators that measured the dispersion of the S_4 surface phonon on Ni(100) employed electron beams with kinetic energy of 180 eV and 320 eV (Szeftel *et al.* 1983). At such high energies, the image potential has very little influence on the electron motion, and experience with the theory of low-energy electron diffraction and angular-resolved photoemission assures us that the calculated cross sections are rather

insensitive to the manner in which electron wavefunctions inside the crystal are joined to those outside. It suffices simply to refract a beam that crosses the crystal–vacuum interface, with deflection controlled by the depth of the inner potential. One may then construct a fully quantitative and predictive theory of electron energy loss cross sections, with knowledge of only the crystal potential experienced by the electron inside the crystal, as outlined above. Note that under circumstances discussed earlier, where the dominant contribution to the excitation cross section comes from the vibration of motion of atoms in the outermost crystal layer, we do *not* require a detailed knowledge of surface lattice dynamics, provided we know the *symmetry* of the atomic motions in the outermost layer, for the mode of interest.

It is evident that the theory of large-angle vibrational losses in electron energy loss spectroscopy has reached the point where fully quantitative and predictive calculations may be made, *provided* one considers impact energies sufficiently large that complications introduced by the image potential may be set aside. Ibach and his colleagues have made experiments with beams of energy sufficiently high for this picture to hold, with the result that for one surface, full contact between theory and experiment has indeed been achieved (Xu *et al.* 1985). It is highly desirable for future experiments to be made in this régime, and we hope to see a shift away from the low energies (1–10 eV) conventionally employed in the studies of near-specular vibrational losses. At such low energies, the high reflectivity of the substrate and the energy variation of the Coulomb excitation cross sections (increasing, as impact energy is lowered) are very favourable for studying near-specular losses, but when one turns to off-specular geometries, the high impact energies greatly simplify interpretation of the data. There are two other reasons why high impact energies are favoured for off-specular studies.

(*a*) The first is purely kinematical. If one wishes to explore the entire two-dimensional Brillouin zone, then high energies are required to achieve the necessary wavevector transfer in the scattering event, if conventional electron spectrometers are employed. If $E^{(i)}$ is the incident electron energy in electronvolts, for quasi-elastic scattering in the geometry illustrated in figure 1, the momentum transfer $Q_{\parallel}$ parallel to the surface is given by

$$Q_{\parallel}\ \mathrm{cm}^{-1} = (E^{(i)})^{\frac{1}{2}}|\sin\theta_i - \sin\theta_s| \times 0.52 \times 10^8. \tag{3.18}$$

In electron energy loss apparatus of conventional design, it is difficult to realize a geometry where the angle between the incident and scattered beam is less than 90°. If we choose $\theta_i = 70°$, $\theta_s = 20°$ as an illustration, then $Q_{\parallel} \approx 0.3 \times 10^8\ (E_i)^{\frac{1}{2}}\ \mathrm{cm}^{-1}$, and energy transfers in the range of several tens of electronvolts are required to excite modes with wavevector at the two-dimensional zone boundary.

(*b*) Our early calculations show that the off-specular scattering efficiencies calculated for excitations of various vibrational modes are very considerably larger in the 100–300 eV range, than they are in the 1–10 eV range (Tong *et al.* 1980). Furthermore, the near-specular dipole cross section is much smaller here. In the low-energy range, where the dipole cross section is large, in the presence of surface imperfections dipole scattering of appreciable strength may be present off-specular and mask the much more feeble impact scattering. This problem is minimized, and higher scattering efficiencies realized off-specular as well, if elevated beam energies are used.

The principal conclusion of this section is that the development of off-specular electron energy loss spectroscopy will be greatly improved if beams in the energy range of 50–300 eV are employed, rather than the low-energy beams commonly used in near-specular studies of dipole

losses. The series of experiments of Ibach & collaborators combined with the set of calculations outlined here, illustrate the power and potential of the method. In the next section of this paper, we discuss in detail a set of specific results obtained from the formalism outlined in the present section.

4. A specific example: the cross section for exciting the S_4 and S_6 surface phonons on the clean N(100) surface

The previous section outlined the formalism that may be used to calculate the cross section of off-specular excitation of surface phonons on clean or adsorbate covered surfaces. Here we discuss a particular set of calculations made by Xu *et al.* (1985). These explore excitation of the S_4 (Rayleigh) surface phonon, and the S_6 surface phonon at the $\bar{X}$ point of the two-dimensional Brillouin zone of a clean Ni(100) surface. We consider two geometries outlined below. In each case, as in the experimental work of Ibach and colleagues, the direction of the scattered beam is held fixed, and as the electron energy is varied, the angle of incidence is varied with electron energy, to fix the wavevector transfer $\boldsymbol{Q}_{\parallel}$ parallel to the surface fixed, and equal to that at the $\bar{X}$ point of the two-dimensional Brillouin zone. The scattering plane contains the $\bar{\Gamma}\bar{X}$ line.

The surface phonons S_4 and S_6 at $\bar{X}$ are on the (100) surface of a f.c.c. crystal are discussed elsewhere, within the framework of a simple analytic theory (see ch. 5 of Ibach & Mills 1982). The S_4 mode has displacements *normal* to the surface in the outermost atomic layer, and in the second layer they are parallel to the surface. As one penetrates into the crystal, one observes alternate parallel and perpendicular displacements, which decay exponentially in magnitude with depth into the crystal. We may denote the displacements in a given layer by a pair of numbers $(u_{\perp}, u_{\parallel})$, the first of which gives the amplitude of the perpendicular component, and the second the parallel component. For S_4, we have the displacements (0.892, 0.00), (0.00, 0.3536), (0.25, 0.00), (0.00, 0.099), (0.07, 0.00) for S_4 in the first five atomic layers. The S_6 mode has displacements *parallel* to the surface in the outermost layer, *perpendicular* in the second layer, with continued alternation between parallel and perpendicular with penetration into the crystal. For the displacements associated with S_6, (0.00, 0.7693), (−0.305, 0.00), (0.00, −0.4315), (0.171, 0.00), (0.00, 0.2418) are the amplitudes in the first five layers. The displacements just quoted assume that the surface and bulk force constants are equal. The S_4 dispersion curve (Szeftel *et al.* 1983) suggests a small stiffening between the force constant that couples the first and second layers. The stiffened force constant has been employed in the calculations compared directly to the data (Xu *et al.* 1985).

The first scattering geometry we consider is one that cannot be realized experimentally with present-day spectrometers. The scattered beam emerges along the surface normal. Figure 3 shows the scattering efficiency per unit solid angle, as defined earlier (Li *et al.* 1980), as a function of incident energy, for exciting S_4 and S_6 at $\bar{X}$. We also show the angle of incidence required to generate the required momentum transfer. The incident beam approaches the crystal near the normal also, so this is near-backscattering geometry. All the electron momentum transfer is thus nearly normal to the surface. If $\Delta k_{\perp}$ is the momentum transfer normal to the surface, and $\Delta k_{\parallel}$ that parallel to it, at 250 eV beam energy, then $\Delta k_{\perp}/\Delta k_{\parallel} = 12.9$. If we estimate the ratio of the S_4 to S_6 cross section at 250 eV by using elementary kinematical arguments, which assume the electrons sample only the thermal motions in the outermost atomic

PHILOSOPHICAL TRANSACTIONS OF THE ROYAL SOCIETY A MATHEMATICAL, PHYSICAL & ENGINEERING SCIENCES

layer, we find S_4 should scatter 225 times more strongly than S_6. In such geometries, where $\Delta k_\perp \gg \Delta k_\parallel$, kinematical estimates show that motions normal to the surface scatter far more strongly than those parallel to it.

The calculations in figure 3 show that indeed, for the whole range of energies explored, the cross section for exciting S_4 is very substantially larger than that for exciting S_6. However, in the 200–300 eV range the ratio of the two cross sections is closer to 50 than to 200. The cross sections in figure 3 have been calculated by synthesizing the scattering amplitude derivatives $(\partial f/\partial R_\beta)$ discussed in §3 from the first layers; here and in all calculations reported in the present paper, the electrons sample the first eighteen layers as they engage in elastic scattering as they approach or exit from the site of the inelastic scattering event. It is of interest to 'take the calculation apart', to see the contribution from atomic vibrations in the various layers. Figure 4 shows that S_4 and S_6 excitation cross section calculated from including only $\partial f/\partial R_\beta$ from the outermost layer, again while the electron samples eighteen layers as it scatters elastically from the crystal. The broken lines in figure 4 show the kinematical estimates of the cross section. Both the S_4 and S_6 results track the kinematical estimates closely on average, except for structure introduced by diffractive scattering of the electron from the crystal, as it approaches or exits from the site of vibrational excitation within the outermost layer. The calculated cross section for excitation of S_4 is in rather close agreement with that displayed in figure 3, while the S_6 cross section is a factor of 4 or 5 smaller, on average, in accord with the kinematical cross section.

Figure 5 shows the S_4 and S_6 cross sections, incorporating now only inelastic scattering from atomic motions in the *second* layer. Recall that the second-layer motion excited by the S_4 mode is parallel to the surface, while the second-layer motion associated with S_6 is *normal* to the surface. Now the S_4 excitation cross section is very much smaller than S_6, and the S_6 cross section is now comparable to that produced by the full cross section calculation displayed in figure 3. The conclusion is that in this near-backscattering geometry, the excitation cross sections are dominated by atomic motions normal to the surface, as expected from kinematical considerations. So one must take due account of the contribution from motions in the *second* layer, to obtain a proper account of the S_6 excitation cross section. In fact, owing to reduced amplitude of the motions excited by S_6 in the second layer, combined with attenuation of the incident and scattered electron beams, the contributions of first- and second-layer motions are comparable and must be synthesized to obtain an adequate description of the cross section. Figure 6 shows excitation cross sections calculated by combining the derivatives $\partial f/\partial R_\beta$ from the first two layers. We see now that cross section for exciting S_6, as provided by the full theory, is nearly reproduced fully.

The message is that in this backscattering geometry, to describe the cross section for exciting S_6, the atomic motions in the second layer as well as the first must be incorporated. This violates the simple scheme outlined in §3, where it is argued that incorporating only $\partial f/\partial R_\beta$ from the first layer should suffice for the computation of the cross section. The geometry considered in the calculations displayed in figures 3–6 is very special, in that *both* the incident and scattered beam propagate very close to the normal to the surface. Under these conditions, multiple scattering *within* an atomic layer parallel to the surface is rather unimportant. This is a consequence of the fact that electron–atom cross sections are rather strongly peaked in the forward direction, in the energy range of interest. As remarked in §3, present electron spectrometers require the angle between the incident and scattered beam to be of the order of 90° or greater. Under these conditions, one or both (incident or scattered) of the electron

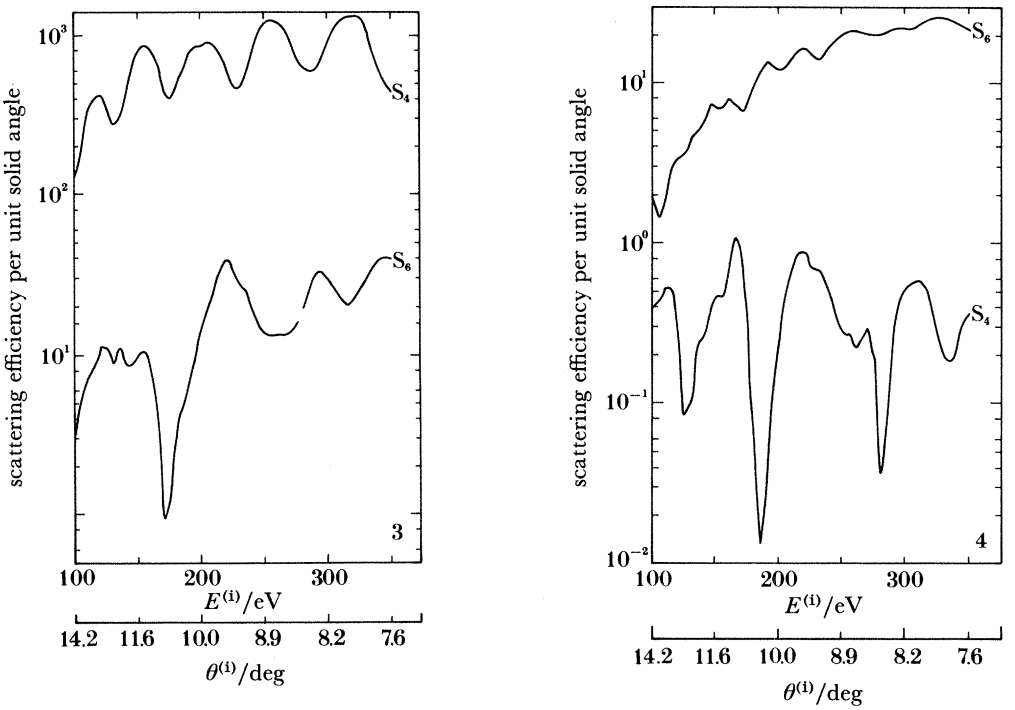

FIGURE 3. Energy variation and magnitude of the cross section for exciting the S_4 and S_6 surface phonon at $\bar{X}$ on the clean Ni(100) surface, for a geometry in which the scattered electron leaves along the surface normal ($\theta^{(s)} = 0$). The cross section is calculated in dimensionless units chosen such that an ordinate of 2000 corresponds to a scattering efficiency of 4×10^{-4}, as defined elsewhere (Li *et al.* 1980). The cross section is calculated by superimposing the derivative $\partial f/\partial R_\beta$ for the first five layers, with the electron allowed to scatter elastically from eighteen layers.

FIGURE 4. The energy variation of the S_4 and S_6 surface-phonon excitation cross sections on Ni(100) at $\bar{X}$, calculated as in figure 3 except that now the only derivative ($\partial f/\partial R_\beta$) retained in the calculation is that from the atomic motions in the outermost atomic layer.

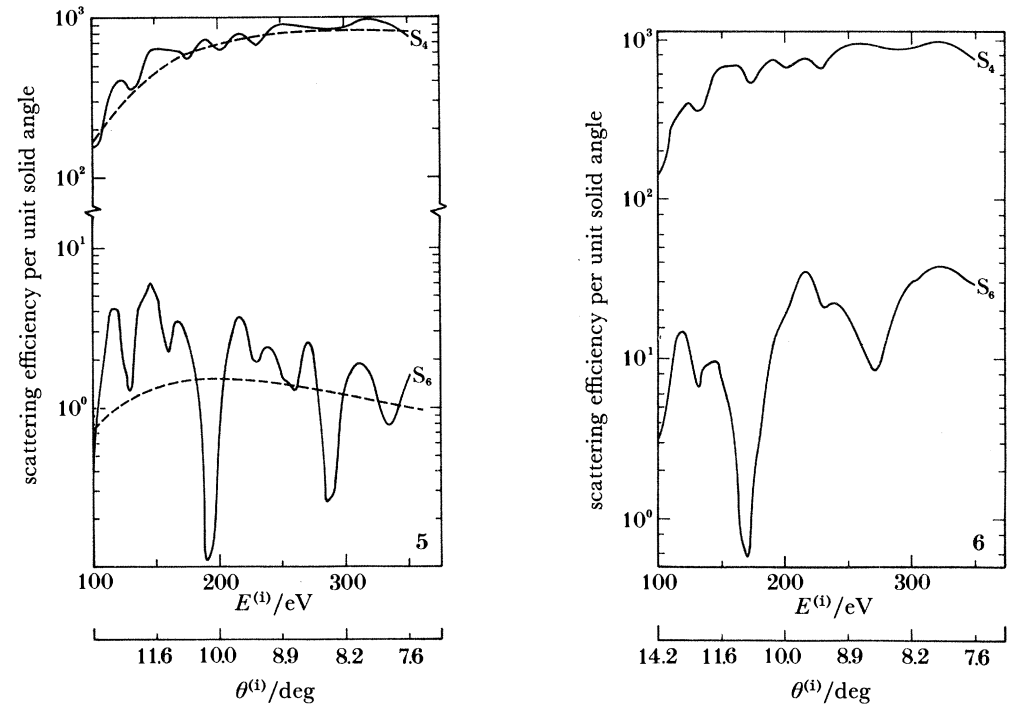

FIGURE 5. The energy variation of the S_4 and S_6 surface-phonon excitation cross sections on Ni(100) at $\bar{X}$, calculated as in figure 3, except the only derivative ($\partial f/\partial R_\beta$) retained in the calculation is that from atom motions in the second layer of atoms.

FIGURE 6. The energy variation of the S_4 and S_6 surface-phonon excitation cross sections on Ni(100) at $\bar{X}$, calculated as in figure 3, but now the cross sections are synthesized by superimposing the scattering amplitude derivatives ($\partial f/\partial R_\beta$) from the outermost two atomic layers.

beams will make a large angle with the normal. When these conditions, applicable to the experiments made to date, are realized, our conclusions are quite different. We now turn to consideration of such a geometry.

In figure 7, we show calculations of the S_4 and S_6 excitation cross section, with all factors held identical to those used to generate figure 3, except for the fact that the scattered electron exists from the crystal at an angle of 72° with respect to the surface normal. This is thus the scattering geometry employed in the first experiment to measure a surface-phonon dispersion curve by the method of inelastic electron scattering (Szeftel *et al.* 1983). It is immediately apparent that while the S_6 cross section is indeed smaller than S_4 over much of the energy range covered in figure 7, nonetheless the contrast in average magnitude is much smaller. There are in fact selected energy ranges where the cross section for S_6 is comparable to or greater than S_4. This theoretical expectation is borne out by the recent experiments of the Ibach group. The calculations reported in figure 7 have been made for an unrelaxed Ni(100) surface. A complete discussion of the sensitivity of the results to details of surface geometry, and a comparison of calculations for a suitably relaxed surface is given elsewhere (Xu *et al.* 1985).

Multiple scattering effects are responsible for enhancing the cross section of S_6 relative to that of S_4, for the geometry considered in figure 7. If either the incident or scattered electron beam make a relatively small angle with respect to the plane of the surface, as the electron enters the crustal, the forward scattering peak in the electron–atom cross section leads to strong multiple scattering within the first atomic layer. The electron can scatter inelastically in such an intra-layer multiple-scattering 'chain' in an event with large momentum transfer parallel to the surface, with the consequence that kinematical theory based on the change in wavevector of the electron calculated from the kinematics of the entering and exiting beams is in *qualitative* error.

If this picture is correct, then we should find that dominant cross section for leaving S_6 is sensitive primarily to atomic motions in the outermost atomic layer, since the parallel motions of the surface atoms may now scatter strongly, by virtue of the intra-layer multiple-scattering events. Figure 8 presents a calculation of the S_4 and S_6 cross sections, retaining only the contribution to the scattering amplitude derivatives $(\partial f/\partial R_\beta)$ from atomic motions within the outermost atomic layer. The results track those in figure 7 remarkably well. Only small differences are evident. Finally, figure 9 shows the cross sections calculated with retention of only the contribution of motions in the second layer. Over the entire energy range, the excitation cross sections are now very much smaller than in figures 7 or 8.

Our conclusion is that under conditions where the incoming or leaving electron beam makes a relatively small angle with the plane of the surface, with the consequence that the electron experiences multiple scattering within the surface layer, even for the S_6 mode with its parallel motions in the surface, the dominant contribution to the excitation cross section comes from motions within the surface layer. The result is that at $\overline{X}$, to within an energy- and angle-dependent normalization factor, the energy variation of the surface-phonon excitation cross sections are controlled principally by the symmetry of the displacement pattern in the outermost layer, and are insensitive to the details of the surface lattice dynamics. In this régime, the theory can be relied upon to provide reliable predictions in the systematics of surface-phonon excitation cross sections. Fortunately, this is the régime where experiments are presently made.

We conclude by emphasizing the role of high impact energies. For beam energies above 50 eV, the theoretical cross sections are insensitive to the details of the electron–surface

PHILOSOPHICAL TRANSACTIONS OF THE ROYAL SOCIETY A MATHEMATICAL, PHYSICAL & ENGINEERING SCIENCES

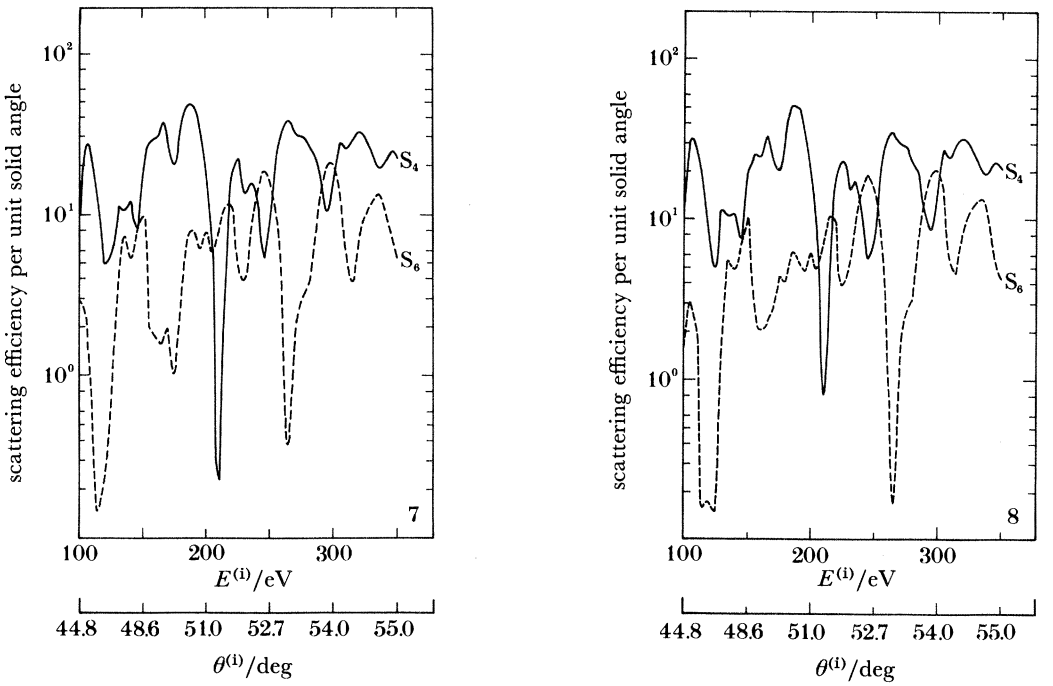

FIGURE 7. For the case where the scattered beam leaves the crystal at an angle of $\theta^{(s)} = 72°$ from the normal, we show the scattering efficiencies for exciting the S_4 and S_6 surface-phonon at $\overline{X}$, on the Ni(100) surface. All factors are held identical to those used to generate figure 3, except for the exit angle.

FIGURE 8. For the scattering geometry used to generate figure 7, we show the excitation cross section calculated in an approximation that retains only the contribution from motion of the outermost layer of the crystal.

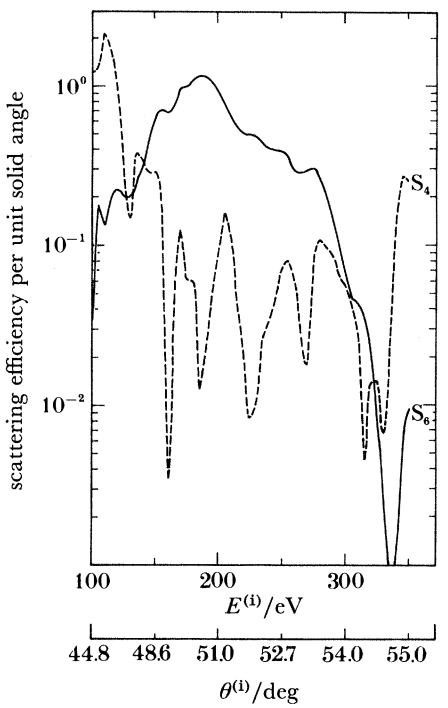

FIGURE 9. For the scattering geometry used to generate figure 7 we show the excitation cross sections calculated in an approximation that retains only the contribution from motion of the outermost layer of the crystal.

interaction such as the image potential, and this allows one to carry through meaningful and quantitative calculations of surface-phonon excitation cross sections, through use of the muffin-tin potentials that form the basis of the theory of low-energy electron diffraction or angular-resolved photoemission. We have one clear case in hand where the theory has provided valuable guidance to experimental studies (Xu *et al.* 1985).

The research of both authors is supported by the U.S. Department of Energy. That of D.L.M. is supported by Grant No. DE-FG-03-84ER-45083, and that of S.Y.T by Grant No. DE-FG-02-84ER-45076.

References

Adnot, A. & Carette, J. D. 1977 *Phys. Rev. Lett.* **38**, 1084.
Baribeau, J. M. & Carette, J. D. 1981*a* *Phys. Rev.* B **23**, 6201.
Baribeau, J. M. & Carette, J. D. 1981*b* *Surf. Sci.* **112**, 241.
Born, M. & Huang, K. 1954 *Dynamical theory of crystal lattices*. Oxford University Press.
Bortolani, V., Franchini, A., Garcia, N., Nizzoli, F. & Santoro, G. 1983 *Phys. Rev.* B **28**, 7358.
Evans, E. & Mills, D. L. 1972 *Phys. Rev.* B **5**, 4126.
Felcher, G. 1981 *Phys. Rev.* B **24**, 1595.
Frenken, J. W. M., van der Veen, J. F. & Allan, G. 1983 *Phys. Rev. Lett.* **51**, 1876.
Gaspari, G. D. & Gyorffy, G. L. 1972 *Phys. Rev. Lett.* **28**, 801.
Greenler, R. G. 1966 *J. chem. Phys.* **44**, 310.
Greenler, R. G. 1969 *J. chem. Phys.* **50**, 1963.
Hall, B. M. 1983 Ph.D. thesis, the University of Wisconsin, Milwaukee.
Hall, B. M., Tong, S. Y. & Mills, D. L. 1983 *Phys. Rev. Lett.* **50**, 1277.
Ho, W., Willis, R. F. & Plummer, E. W. 1978 *Phys. Rev. Lett.* **40**, 1463.
Ho, W., Willis, R. F. & Plummer, E. W. 1980 *Phys. Rev.* B **21**, 4202.
Ibach, H. & Mills, D. L. 1982 *Electron energy loss spectroscopy and surface vibrations*. San Francisco: Academic Press.
Lehwald, S., Szeftel, J. M., Ibach, H., Rahman, T. S. & Mills, D. L. 1983 *Phys. Rev. Lett.* **50**, 518.
Li, C. H., Tong, S. Y. & Mills, D. L. 1980 *Phys. Rev.* B **21**, 3057.
Rahman, T. S. & Ibach, H. 1985 *Phys. Rev. Lett.* **54**, 1933.
Rahman, T. S., Mills, D. L. & Black, J. E. 1983*a* *Phys. Rev.* B **27**, 4059.
Rahman, T. S., Mills, D. L. & Black, J. E. 1983*b* *J. Electron Spectrosc. rel. Phen.* **27**, 199.
Rahman, T. S., Mills, D. L., Szeftel, J. M., Lehwald, S. & Ibach, H. 1984 *Phys. Rev.* B **30**, 589.
Roundy, V. & Mills, D. L. 1972 *Phys. Rev.* B **5**, 1347.
Szeftel, J. M., Lehwald, S., Ibach, H., Rahman, T. S., Black, J. E. & Mills, D. L. 1983 *Phys. Rev. Lett.* **51**, 268.
Toennies, J. P. 1984 *J. Vac. Sci. Technol.* A **2**, 1055.
Tong, S. Y. 1975 *Prog. Surf. Sci.* **7**, 1.
Tong, S. Y., Li, C. H. & Mills, D. L. 1980 *Phys. Rev. Lett.* **44**, 407.
Tong, S. Y., Li, C. H. & Mills, D. L. 1981 *Phys. Rev.* B **24**, 806.
Wallis, R. F. 1973 *Prog. Surf. Sci.* **4**, 233.
Willis, R. F. 1979 *Surf. Sci.* **89**, 457.
Xu, M. L., Hall, B. M., Tong, S. Y., Rocca, M., Ibach, H. & Lehwald, S. 1985 *Phys. Rev. Lett.* **54**, 1171.

PHILOSOPHICAL TRANSACTIONS OF THE ROYAL SOCIETY A MATHEMATICAL, PHYSICAL & ENGINEERING SCIENCES